

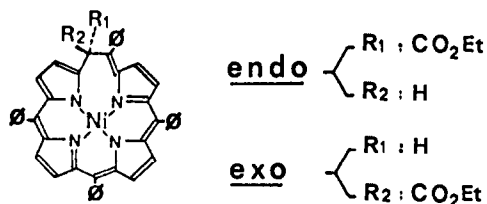
# A New Homoporphyrin System. The 21-Ethoxycarbonyl-5,10,15,20-tetraphenyl-21*H*-21-homoporphine. Crystal Structure and Molecular Stereochemistry of the Nickel(II) Complex

Bernard Chevrier and Raymond Weiss\*

Contribution from the Institut de Chimie, Laboratoire de Cristalochimie associé au C.N.R.S., Université Louis Pasteur, BP 296/R8, Strasbourg, France. Received July 22, 1974

**Abstract:** The nickel(II) complex of the 21-ethoxycarbonyl-5,10,15,20-tetraphenyl-21*H*-21-homoporphine exists as two thermally stable epimers, endo and exo. The structure of the endo epimer has been determined from three-dimensional X-ray counter data. This epimer crystallizes in the triclinic system as the dichloromethane solvate, space group  $P\bar{1}$ . The unit cell has  $a = 17.773(4) \text{ \AA}$ ,  $b = 13.064(3) \text{ \AA}$ ,  $c = 13.414(3) \text{ \AA}$ ,  $\alpha = 126.88(4)^\circ$ ,  $\beta = 73.14(3)^\circ$ , and  $\gamma = 125.68(2)^\circ$  and contains two molecules. The structure was solved by Patterson and Fourier methods, and refined by least-squares techniques to conventional and weighted discrepancy factors of 0.073 and 0.102, respectively, for the 5516 reflections having  $I > 4\sigma_I$ . The structure consists of well-separated molecules. The nickel atom exhibits square-planar coordination, involving nitrogen atoms of the four pyrrole bases. One of the Ni-N bond lengths, 1.961(3) Å, is longer than the other three which are equal to  $1.886 \pm 0.010 \text{ \AA}$ . The macrocyclic ligand is highly distorted. Individual pyrrole rings are planar but are rotated with respect to the four nitrogen least-squares plane. The angles between the planes of adjacent pyrroles are 39.8, 38.3, 29.6 and 73.4°. The distortion appears as a result of the ester carbon insertion in the chain between two pyrroles of the original tetraphenylporphine. This provides a ring expansion which also affects the Ni-N bond lengths. This work describes the first example of a homoporphyrin complex structure.

In the last few years extensive works have appeared with regard to porphyrins and metalloporphyrins.<sup>1-3</sup> Even without their biological and industrial implications, the properties of metalloporphyrins would be studied for their purely theoretical importance. Recently a new macrocycle derived from tetraphenylporphine by successive chemical steps has been synthesized.<sup>4</sup> This was isolated as its nickel(II) complex in the form of two thermally stable epimers, endo and exo. Based on their spectroscopic and chemical behavior, these epimers, presumed to be homoporphyrins, were ascribed the following structures.



An essential characteristic of porphyrins is the existence of an aromatic conjugated system. In these last new compounds the ring expansion by a saturated carbon atom involves distortions of the macrocycle and accordingly modifications in the  $\pi$ -delocalized system. The only compound of this type so far described is an azahomoporphyrin,<sup>5</sup> but unfortunately this last compound was unstable and rearranged to a usual porphyrin. Thus, it appeared of great interest to specify the unknown geometry of such compounds. Hence we established the crystal structure of the present compound.<sup>6</sup>

## Experimental Section

Single crystals were grown by slow evaporation from a nitromethane-dichloromethane solution. Preliminary X-ray studies of the exo epimer established a four-molecule unit cell in the monoclinic space group  $P2_1/c$ . Approximate lattice constants are  $a = 12.17 \text{ \AA}$ ,  $b = 10.00 \text{ \AA}$ ,  $c = 34.31 \text{ \AA}$ ,  $\beta = 101.3^\circ$ , and  $V = 4095 \text{ \AA}^3$ . This monoclinic form was not characterized further. Indeed the

fact that the visible absorption spectra of both epimers are quite similar suggests an identical conjugated system.<sup>4</sup> Accordingly only the structural study of the endo crystals was carried out. Preliminary precession photographs of the endo epimer showed only the required center of symmetry and hence the space group is either  $P1$  or  $P\bar{1}$ . The triclinic cell dimensions were subsequently adjusted by least-squares refinement of the setting angles of 12 reflections measured on a Picker four-circle automatic diffractometer with Mo  $K\alpha$  radiation ( $\lambda 0.70926 \text{ \AA}$ ) using the method outlined by Busing:<sup>7</sup>  $a = 17.773(4) \text{ \AA}$ ,  $b = 13.064(3) \text{ \AA}$ ,  $c = 13.414(3) \text{ \AA}$ ;  $\alpha = 126.88(4)^\circ$ ,  $\beta = 73.14(3)^\circ$ ,  $\gamma = 125.68(2)^\circ$ ;  $V = 2015 \text{ \AA}^3$ . The calculated density based on two molecules ( $\text{C}_{48}\text{H}_{34}\text{N}_4\text{O}_2\text{Ni}$ ,  $M = 757.5$ ) per unit cell is  $1.248 \text{ g/cm}^3$ . As measured by flotation in aqueous calcium chloride solution, the density of crystals freshly taken from solutions is  $1.29 \text{ g/cm}^3$ . However, this observed density rapidly decreases to  $1.25 \text{ g/cm}^3$  in a few days. It suggests that crystals contain small amounts of occluded solvent. A unit cell content of two molecules of complex and one  $\text{CH}_2\text{Cl}_2$  molecule requires a calculated density of  $1.318 \text{ g/cm}^3$ . This is close to the above-mentioned density of freshly prepared crystals.

For data collection, a suitable crystal cut to a spherical shape of about 0.28 mm in diameter was selected, sealed in a Lindeman glass tube, and mounted on the diffractometer. The data were collected in the range  $5 < 2\theta < 60^\circ$  by the  $\theta$ - $2\theta$  scan method at  $18 \pm 2^\circ$  using graphite-monochromated Mo  $K\alpha$  radiation. Background counts were taken for 20 sec at each end of the scan range, and a scan rate of  $2^\circ$  in  $2\theta$  per minute was used. The scan range was  $1.8^\circ$ . Attenuators were automatically inserted if the intensity of the diffracted beam exceeded 7000 counts per second during a scan. Of the independent reflections measured out to a  $\sin \theta/\lambda$  of 0.71, all reflections having a net intensity smaller than  $4\sigma I$  were taken to be unobserved; 5516 independent data were coded as observed (46% of the theoretical number possible). The standard deviation  $\sigma I$  was defined in terms of the statistical variances of the

$$\sigma I^2 = CT + (Tc/Tb)^2(B1 + B2) + (pI)^2$$

counts as where  $CT$  is the total scan count,  $B1$  and  $B2$  are background counts,  $Tc$  and  $Tb$  are respectively scan and background times, and  $p$  is an empirical coefficient of the net count  $I$ .<sup>8</sup> An initial value of 0.05 was used for  $p$ .

During the course of the intensity data collection, the intensities of three reflections (900,150,0 $\bar{1}$ 5) were monitored as a function of X-ray exposure to the crystal. The standard deviations from the average intensities for 202 measurements of the monitor reflec-

Table I. Fractional Atomic Coordinates<sup>a</sup>

Atom	x	y	z
Ni	0.21164 (3)	0.07992 (6)	0.21613 (4)
N1	0.2313 (2)	0.1274 (4)	0.3735 (3)
C11	0.2821 (2)	0.1012 (5)	0.4017 (3)
C12	0.2870 (3)	0.1674 (6)	0.5331 (4)
C13	0.2362 (3)	0.2323 (6)	0.5836 (3)
C14	0.1996 (2)	0.2049 (5)	0.4843 (3)
N2	0.0905 (2)	0.0400 (3)	0.2561 (2)
C21	0.0673 (2)	0.1208 (4)	0.3743 (3)
C22	-0.0258 (3)	0.0774 (5)	0.3652 (4)
C23	-0.0604 (3)	-0.0331 (5)	0.2454 (4)
C24	0.0133 (2)	-0.0531 (4)	0.1774 (3)
N3	0.1798 (2)	0.0057 (3)	0.0535 (3)
C31	0.0928 (2)	-0.1063 (4)	-0.0117 (3)
C32	0.1009 (3)	-0.1535 (5)	-0.1408 (3)
C33	0.1897 (3)	-0.0617 (5)	-0.1497 (3)
C34	0.2395 (2)	0.0377 (4)	-0.0286 (3)
N4	0.3442 (2)	0.1651 (3)	0.1896 (3)
C41	0.3800 (2)	0.2165 (4)	0.1133 (3)
C42	0.4775 (3)	0.3328 (5)	0.1506 (4)
C43	0.5022 (2)	0.3444 (5)	0.2429 (4)
C44	0.4207 (2)	0.2326 (4)	0.2653 (3)
C5	0.4242 (2)	0.1790 (4)	0.3241 (3)
C51	0.5094 (2)	0.2504 (5)	0.3960 (3)
C52	0.5651 (3)	0.4041 (5)	0.4818 (4)
C53	0.6466 (3)	0.4644 (5)	0.5419 (4)
C54	0.6712 (3)	0.3703 (6)	0.5170 (4)
C55	0.6164 (3)	0.2173 (6)	0.4331 (5)
C56	0.5369 (3)	0.1570 (5)	0.3740 (4)
C6	0.1227 (2)	0.2106 (4)	0.4852 (3)
C61	0.0950 (2)	0.3004 (4)	0.6077 (3)
C62	0.0253 (3)	0.2335 (5)	0.6665 (4)
C63	0.0007 (4)	0.3218 (7)	0.7818 (5)
C64	0.0464 (4)	0.4719 (7)	0.8381 (4)
C65	0.1158 (4)	0.5403 (6)	0.7824 (5)
C66	0.1414 (4)	0.4546 (6)	0.6676 (5)
C7	0.0104 (2)	-0.1418 (4)	0.0449 (3)
C71	-0.0804 (2)	-0.2532 (4)	-0.0284 (3)
C72	-0.1068 (3)	-0.2352 (5)	-0.1021 (4)
C73	-0.1927 (3)	-0.3374 (5)	-0.1686 (4)
C74	-0.2555 (3)	-0.4605 (6)	-0.1609 (5)
C75	-0.2319 (3)	-0.4822 (6)	-0.0880 (5)
C76	-0.1457 (3)	-0.3798 (6)	-0.0213 (5)
C8	0.3333 (2)	0.1530 (4)	0.0037 (3)
C81	0.3836 (3)	0.2002 (5)	-0.0839 (3)
C82	0.4567 (8)	0.1843 (5)	-0.1414 (4)
C83	0.5031 (3)	0.2240 (3)	-0.2241 (1)
C84	0.4723 (4)	0.2823 (6)	-0.2544 (5)
C85	0.3990 (4)	0.3019 (6)	-0.1964 (5)
C86	0.3554 (3)	0.2599 (6)	-0.1127 (4)
C1	0.3390 (3)	0.0381 (5)	0.3141 (4)
C2	0.2955 (3)	-0.0979 (5)	0.1828 (4)
O1	0.2150 (2)	-0.1771 (4)	0.1477 (3)
O2	0.3600 (2)	-0.1190 (4)	0.1105 (3)
C3	0.3330 (4)	-0.2374 (6)	-0.0226 (5)
C4	0.3621 (5)	-0.1671 (8)	-0.0924 (6)
Solvate atom			
C9	0.1138 (13)	-0.3677 (24)	0.3700 (15)
C11	0.2121 (5)	-0.2085 (7)	0.4524 (7)
C12	0.0757 (7)	-0.4476 (14)	0.4712 (10)

<sup>a</sup> Numbers in parentheses here and in succeeding tables are estimated standard deviations in the last significant figure.

tions were 2.1, 1.9, and 1.9%. Thus, the crystal showed no loss in intensity due to exposure, the intensity of the X-ray source was constant for practical purposes, and the crystal remained well aligned throughout the data collection.

The 5516 recorded intensities were corrected for Lorentz and polarization effects. The small linear absorption coefficient ( $\mu = 5.2 \text{ cm}^{-1}$ ) indicated absorption effects could be neglected. Only these observed data were used for the determination and refinement of structure.

The choice of  $P\bar{1}$  as the space group rather than  $P1$  was confirmed by the successful solution of the structure. The coordinates of the two nickel atoms lying in general positions were obtained by

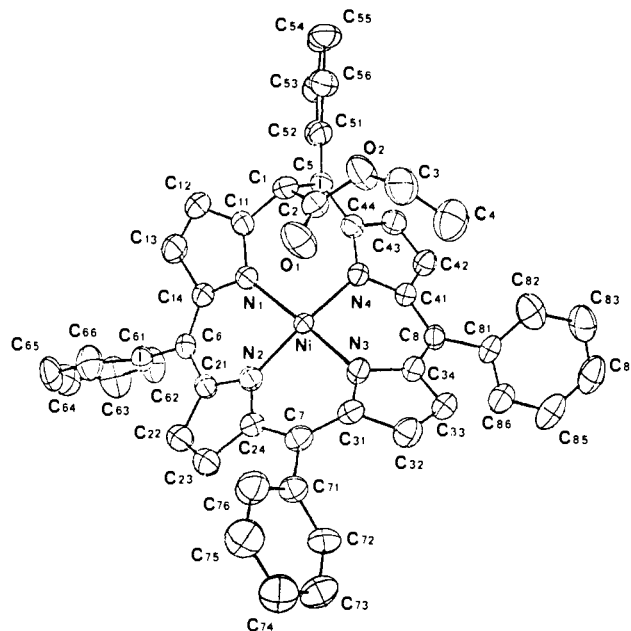


Figure 1. Perspective view of the nickel-homoporphyrin molecule as it exists in the crystal. Also displayed is the atomic labeling scheme used throughout the paper.

inspection of the three-dimensional Patterson synthesis. Using the calculated contributions of nickel to determine phases, the Fourier synthesis gave positions for all nonhydrogen atoms.

The effects of anomalous dispersion were included for the nickel atom by use of  $\Delta f'$  and  $\Delta f''$  values given in the ref 9. The atomic scattering factors were those tabulated by Cromer and Waber.<sup>10</sup> Nickel was assumed to be in the zero ionization state.

Refinement by a full-matrix least-squares procedure<sup>11</sup> with isotropic thermal parameters for individual atoms led to the conventional index

$$R_1 = \frac{\sum ||F_o| - |F_c||}{\sum |F_o|} = 0.142$$

All refinements were carried out on  $F_o$ ; the function minimized was  $\sum w(|F_o| - |F_c|)^2$ ; the weight  $w$  was taken as  $1/\sigma^2(F_o)$ .

At this stage of resolution, a difference Fourier synthesis revealed electron density concentrations appropriately located for hydrogen atoms and electronic residues attributable to a  $\text{CH}_2\text{Cl}_2$  molecule present as uncomplexed solvent of crystallization. The hydrogen atoms were fixed in the theoretically calculated positions ( $\text{C}-\text{C}-\text{H}$ ,  $109.5^\circ$ ;  $\text{C}-\text{H}$ ,  $1.0 \text{ \AA}$ ), included in the subsequent refinements, but not refined. These were assigned isotropic temperature factors using the expression  $B_H = B_C + 1.0$ . Because of computer memory limitations, the overall structure was then refined by anisotropic block-diagonal least-squares analysis. A  $p$  value of 0.09 was used in the last cycles of refinement. The final value of  $R_1$  was 0.073, that of the weighted index

$$R_2 = \frac{[\sum w(|F_o| - |F_c|)^2 / \sum w |F_o|^2]^{1/2}}$$

was 0.102. The estimated standard deviation of an observation of unit weight was 1.7. A final difference Fourier map revealed no other peaks higher than  $0.5 \text{ e}/\text{\AA}^3$ , with the exception of a  $1.7 \text{ e}/\text{\AA}^3$  maxima located close to the  $\text{CH}_2\text{Cl}_2$  molecule.

The solvate nearby the inversion center of space group  $P\bar{1}$  is only present as a half-molecule per asymmetric unit cell. Both the Fourier synthesis of electron density and the extraordinarily large thermal parameters of the  $\text{CH}_2\text{Cl}_2$  atoms suggest incomplete occupancy of the positions assigned to solvent molecules. However, the parameters describing the complex ligand were found to be essentially invariant to incorporation of solvent into the structure model and to changes in the parameters describing the solvent molecules. The high values of the  $R_1$  and  $R_2$  discrepancy indexes probably arise in part from this not well-defined solvate position.

Atomic coordinates and the associated anisotropic thermal parameters are listed in Tables I and II, respectively. A table of observed and calculated structure factors is available.<sup>12</sup>

**Table II.** Anisotropic Thermal Parameters ( $\text{\AA}^2$ )<sup>a</sup>

Atom	$B_{11}$	$B_{22}$	$B_{33}$	$B_{12}$	$B_{13}$	$B_{23}$
Ni	2.4 (0)	3.2 (0)	2.1 (0)	1.5 (0)	0.2 (0)	1.5 (0)
N1	3.0 (1)	4.1 (2)	2.9 (1)	2.1 (1)	0.5 (1)	2.0 (1)
C11	3.3 (2)	4.4 (2)	3.1 (2)	2.1 (2)	0.6 (1)	2.3 (2)
C12	4.6 (2)	6.9 (3)	3.5 (2)	3.2 (2)	0.6 (2)	3.3 (2)
C13	4.1 (2)	6.2 (3)	2.4 (2)	2.9 (2)	0.6 (2)	2.1 (2)
C14	3.2 (2)	4.2 (2)	2.8 (2)	2.1 (2)	0.7 (1)	2.2 (2)
N2	3.0 (1)	3.2 (1)	2.7 (1)	1.5 (1)	0.1 (1)	1.6 (1)
C21	2.9 (2)	3.5 (2)	3.0 (2)	1.8 (1)	0.5 (1)	1.8 (2)
C22	3.7 (2)	5.0 (2)	3.9 (2)	2.6 (2)	0.5 (2)	2.3 (2)
C23	3.4 (2)	5.4 (2)	4.0 (2)	2.6 (2)	0.6 (2)	2.7 (2)
C24	3.1 (2)	3.5 (2)	3.2 (2)	1.6 (2)	0.2 (1)	2.1 (2)
N3	2.9 (1)	3.3 (1)	2.7 (1)	1.5 (1)	0.3 (1)	1.8 (1)
C31	3.3 (2)	3.2 (2)	3.0 (2)	1.5 (2)	-0.1 (1)	1.8 (1)
C32	4.0 (2)	3.8 (2)	2.8 (2)	1.9 (2)	-0.1 (1)	1.5 (2)
C33	4.0 (2)	4.7 (2)	2.9 (2)	2.2 (2)	0.3 (1)	2.3 (2)
C34	3.5 (2)	3.8 (2)	2.4 (2)	2.0 (2)	0.2 (1)	1.7 (1)
N4	2.9 (1)	3.4 (1)	2.8 (1)	1.6 (1)	0.3 (1)	1.9 (1)
C41	2.9 (2)	3.2 (2)	2.6 (2)	1.7 (1)	0.3 (1)	1.6 (1)
C42	3.6 (2)	3.6 (2)	3.3 (2)	1.5 (2)	0.2 (1)	2.1 (2)
C43	2.5 (2)	4.0 (2)	3.8 (2)	1.3 (2)	0.0 (1)	2.2 (2)
C44	3.0 (2)	3.7 (2)	2.7 (2)	2.0 (1)	0.4 (1)	1.6 (1)
C5	2.7 (2)	3.7 (2)	2.9 (2)	1.8 (1)	0.3 (1)	1.8 (1)
C51	3.3 (2)	4.4 (2)	3.0 (2)	2.2 (2)	0.2 (1)	2.1 (2)
C52	4.6 (2)	4.8 (2)	3.0 (2)	2.9 (2)	-0.0 (2)	1.8 (2)
C53	4.0 (2)	4.4 (2)	4.0 (2)	1.5 (2)	-0.8 (2)	1.9 (2)
C54	4.1 (2)	6.5 (3)	4.1 (2)	3.0 (2)	-0.2 (2)	2.8 (2)
C55	4.8 (3)	5.9 (3)	5.3 (2)	3.4 (2)	-0.2 (2)	2.9 (2)
C56	4.6 (2)	5.0 (2)	4.3 (2)	3.0 (2)	0.2 (2)	2.3 (2)
C6	3.2 (2)	3.4 (2)	2.9 (2)	1.8 (1)	0.7 (1)	1.8 (1)
C61	3.0 (2)	3.8 (2)	2.7 (2)	1.9 (2)	0.6 (1)	1.7 (1)
C62	5.5 (3)	4.3 (2)	4.5 (2)	2.7 (2)	1.9 (2)	2.7 (2)
C63	6.0 (3)	6.7 (3)	4.4 (2)	4.0 (2)	2.9 (2)	3.4 (2)
C64	6.6 (3)	6.4 (3)	3.4 (2)	4.5 (3)	0.9 (2)	1.8 (2)
C65	6.5 (3)	4.5 (2)	4.3 (3)	3.0 (2)	1.4 (2)	1.5 (2)
C66	5.4 (3)	4.5 (3)	4.4 (2)	2.5 (2)	1.4 (2)	2.4 (2)
C7	2.8 (2)	3.2 (2)	3.3 (2)	1.2 (1)	-0.3 (1)	1.8 (2)
C71	2.9 (2)	3.1 (2)	3.2 (2)	1.1 (2)	-0.5 (1)	1.5 (2)
C72	4.2 (2)	3.6 (2)	4.1 (2)	1.9 (2)	-0.6 (2)	1.9 (2)
C73	4.5 (2)	4.1 (2)	4.2 (2)	1.8 (2)	-1.2 (2)	1.8 (2)
C74	3.7 (2)	4.4 (3)	4.6 (3)	1.1 (2)	-1.1 (2)	1.5 (2)
C75	3.6 (2)	4.9 (3)	5.8 (3)	4 (2)	-0.7 (2)	3.4 (2)
C76	3.9 (2)	4.6 (3)	5.0 (3)	1.2 (2)	-0.4 (2)	3.1 (2)
C8	3.2 (2)	3.4 (2)	2.8 (2)	1.9 (2)	0.6 (1)	2.0 (2)
C81	4.0 (2)	3.4 (2)	2.7 (2)	1.6 (2)	0.2 (1)	1.9 (2)
C82	5.6 (1)	3.1 (1)	3.3 (2)	3.7 (2)	0.3 (1)	1.0 (2)
C83	2.2 (1)	5.9 (3)	5.7 (3)	.8 (2)	1.4 (2)	4.0 (2)
C84	5.6 (3)	5.6 (3)	4.5 (3)	1.2 (2)	0.3 (2)	3.6 (2)
C85	7.0 (3)	5.1 (3)	4.3 (2)	2.1 (3)	-0.3 (2)	3.2 (2)
C86	5.4 (3)	4.9 (3)	3.6 (2)	2.7 (2)	0.2 (2)	2.6 (2)
C1	3.3 (2)	4.5 (2)	3.4 (2)	2.2 (2)	0.5 (1)	2.6 (2)
C2	3.3 (2)	4.4 (2)	4.4 (2)	2.1 (2)	0.8 (2)	2.9 (2)
O1	3.4 (2)	4.8 (2)	5.9 (2)	1.6 (1)	0.0 (1)	1.9 (2)
O2	4.2 (2)	5.5 (2)	4.1 (2)	2.8 (1)	0.7 (1)	1.7 (1)
C3	6.6 (3)	5.5 (3)	3.8 (2)	3.8 (3)	1.0 (2)	2.0 (2)
C4	7.5 (4)	7.1 (4)	5.1 (3)	4.0 (3)	0.6 (3)	3.0 (3)
C9	9.3 (1.1)	10.7 (1.3)	4.9 (8)	8.4 (1.1)	-2.5 (8)	-1.8 (8)
C11	12.4 (4)	8.7 (3)	13.6 (5)	5.9 (3)	-1.6 (4)	5.5 (3)
C12	17.4 (8)	20.9 (1.0)	15.6 (8)	10.5 (8)	2.5 (6)	9.7 (7)

<sup>a</sup> The  $B_{ij}$  are related to the dimensionless  $\beta_{ij}$  used during refinement as  $B_{ij} = 4\beta_{ij}/a_i^*a_j^*$ .

## Results and Discussion

The numbering system used in Tables I–VI for the carbon, nitrogen, and oxygen atoms in the nickel-homoporphyrin molecule is displayed in Figure 1. A stereoscopic view of the molecule is drawn in Figure 2 with the same relative orientation as Figure 1. Table III contains a list of intramolecular bond lengths and angles.

There are several interesting points that have resulted from this work. One is that this metallohomoporphyrin is not a planar molecule. The nonplanarity can be described in the following manner. Pyrrole rings are separately planar but are rotated with respect to the four nitrogen least-squares (4N) plane. The angles between the (4N) plane and

the planes of each of the N(1) to N(4) pyrrole nuclei are 43.6, 31.9, 24.0, and 33.4°. Equations of the planes referred to the axial system  $\mathbf{a}, \mathbf{c}^*\Lambda\mathbf{a}, \mathbf{c}^*$  were calculated according to the method of Schomaker, *et al.*<sup>13</sup> For comparison, the distances of the respective atoms from these planes are given in Table IV. The displacements of the homoporphine skeletal atoms from the (4N) plane are also displayed in Figure 3.

Of particular interest is the large angle of 73.4° between the N(1) and N(4) pyrrole planes. Previous structural determinations have generally shown that smaller departures from planarity are observed for the porphinato core in porphyrins and metalloporphyrins.<sup>1,14–21</sup> Most so-called planar porphyrins have angles between adjacent pyrrole groups in

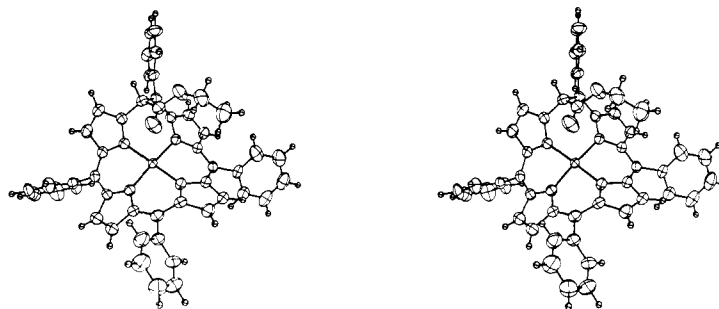


Figure 2. Computer-drawn model in perspective of the nickel-homoporphyrin molecule. Nonhydrogen atoms are drawn at their 50% probability ellipsoids. The hydrogen atoms have been drawn artificially small.

Table III. Intramolecular Bond Lengths and Angles

Bond Lengths, Å							
Ni-N1	1.889 (4)	C5-C1	1.506 (6)	C32-C33	1.341 (5)	C7-C24	1.420 (5)
Ni-N2	1.883 (4)	C5-C44	1.363 (10)	C33-C34	1.437 (6)	C7-C31	1.387 (6)
Ni-N3	1.885 (4)	C5-C51	1.486 (7)	C34-N3	1.369 (5)	C7-C71	1.469 (6)
Ni-N4	1.961 (3)	C51-C52	1.381 (5)	N4-C41	1.362 (7)	C71-C72	1.389 (11)
N1-C11	1.336 (10)	C52-C53	1.397 (9)	C41-C42	1.443 (5)	C72-C73	1.375 (7)
C11-C12	1.427 (7)	C53-C54	1.366 (13)	C42-C43	1.326 (10)	C73-C74	1.371 (9)
C12-C13	1.356 (11)	C54-C55	1.369 (6)	C43-C44	1.459 (6)	C74-C75	1.387 (14)
C13-C14	1.409 (10)	C55-C56	1.359 (10)	C44-N4	1.409 (7)	C75-C76	1.381 (7)
C14-N1	1.388 (5)	C56-C51	1.413 (11)			C76-C71	1.406 (8)
N2-C21	1.385 (5)	C6-C14	1.408 (9)	C1-C11	1.485 (7)	C8-C34	1.394 (5)
C21-C22	1.421 (8)	C6-C21	1.402 (6)	C1-C2	1.513 (5)	C8-C41	1.407 (7)
C22-C23	1.342 (6)	C6-C61	1.487 (5)	C2-O1	1.190 (5)	C8-C81	1.477 (7)
C23-C24	1.428 (7)	C61-C62	1.384 (7)	C2-O2	1.317 (6)	C81-C82	1.368 (14)
C24-N2	1.353 (5)	C62-C63	1.404 (7)	O2-C3	1.459 (5)	C82-C83	1.357 (7)
N3-C31	1.382 (4)	C63-C64	1.340 (9)	C3-C4	1.478 (14)	C83-C84	1.425 (13)
C31-C32	1.442 (6)	C64-C65	1.363 (9)	C9-C11	1.651 (16)	C84-C85	1.390 (10)
		C65-C66	1.396 (8)	C9-C12	1.932 (36)	C85-C86	1.379 (10)
		C66-C61	1.374 (7)			C86-C81	1.391 (12)
Bond Angles, deg							
N1-Ni-N2	87.7 (1)	C1-C5-C51	117.4 (4)	N2-C24-C7	124.3 (4)	C7-C71-C76	120.0 (5)
N2-Ni-N3	88.9 (1)	C1-C5-C44	119.1 (4)	C7-C24-C23	124.8 (5)	C71-C72-C73	122.2 (5)
N3-Ni-N4	91.8 (1)	C44-C5-C51	123.3 (4)			C72-C73-C74	119.4 (6)
N4-Ni-N1	92.8 (1)	C5-C51-C52	123.9 (5)	Ni-N3-C31	126.3 (2)	C73-C74-C75	120.0 (6)
N1-Ni-N3	172.2 (2)	C5-C51-C56	118.6 (5)	Ni-N3-C34	127.0 (2)	C74-C75-C76	120.6 (6)
N2-Ni-N4	167.6 (2)	C51-C52-C53	121.0 (5)	N3-C31-C32	109.2 (4)	C75-C76-C71	119.8 (5)
		C52-C53-C54	119.8 (6)	C31-C32-C33	106.9 (5)	C76-C71-C72	117.7 (5)
		C53-C54-C55	120.1 (6)	C32-C33-C34	107.6 (5)		
Ni-N1-C11	127.2 (3)	C54-C55-C56	120.6 (6)	C33-C34-N3	109.6 (4)	C34-C8-C41	120.9 (4)
Ni-N1-C14	125.8 (2)	C55-C56-C51	121.0 (5)	C34-N3-C31	106.1 (4)	C34-C8-C81	118.0 (4)
N1-C11-C12	109.8 (5)	C56-C51-C52	117.3 (5)	N3-C31-C7	123.7 (4)	C41-C8-C81	120.9 (4)
C11-C12-C13	107.0 (5)			C7-C31-C32	125.6 (5)	C8-C81-C82	122.1 (6)
C12-C13-C14	107.0 (5)	C14-C6-C21	120.7 (4)	N3-C34-C8	124.0 (4)	C8-C81-C86	119.9 (5)
C13-C14-N1	109.1 (4)	C14-C6-C61	118.6 (4)	C8-C34-C33	126.3 (5)	C81-C82-C83	123.4 (7)
C14-N1-C11	106.8 (4)	C21-C6-C61	120.3 (4)			C82-C83-C84	118.0 (7)
N1-C11-C1	124.9 (4)	C6-C61-C62	121.6 (5)	Ni-N4-C41	120.0 (2)	C83-C84-C85	119.9 (6)
C1-C11-C12	124.3 (5)	C6-C61-C66	119.9 (5)	Ni-N4-C44	130.5 (2)	C84-C85-C86	118.9 (6)
N1-C14-C6	121.8 (4)	C61-C62-C63	120.0 (6)	N4-C41-C42	110.1 (4)	C85-C86-C81	121.8 (6)
C6-C14-C13	126.3 (5)	C62-C63-C64	120.4 (6)	C41-C42-C43	107.6 (4)	C86-C81-C82	117.8 (7)
		C63-C64-C65	120.4 (7)	C42-C43-C44	107.8 (4)		
Ni-N2-C21	124.8 (2)	C64-C65-C66	120.1 (7)	C43-C44-N4	107.7 (4)	C2-C1-C5	115.8 (4)
Ni-N2-C24	128.4 (2)	C65-C66-C61	120.4 (6)	C44-N4-C41	105.8 (4)	C2-C1-C11	117.9 (4)
N2-C21-C22	109.1 (4)	C66-C61-C62	118.4 (6)	N4-C41-C8	125.4 (4)	C5-C1-C11	99.9 (4)
C21-C22-C23	107.6 (5)			C8-C41-C42	123.9 (4)	C1-C2-O1	126.2 (5)
C22-C23-C24	106.8 (5)	C24-C7-C31	119.3 (4)	N4-C44-C5	126.0 (4)	C1-C2-O2	110.0 (4)
C23-C24-N2	110.2 (4)	C24-C7-C71	118.5 (4)	C5-C44-C43	124.0 (4)	O1-C2-O2	123.7 (5)
C24-N2-C21	106.0 (4)	C31-C7-C71	121.4 (4)			C2-O2-C3	118.3 (5)
N2-C21-C6	123.9 (4)	C7-C71-C72	122.1 (5)	C11-C9-C12	99 (1)	O2-C3-C4	109.1 (6)
C6-C21-C22	126.1 (5)						

the range of 2–6°. Important deformations were recently found for a nonmetallo N-substituted octaethylporphyrin<sup>22</sup> and for the tetragonal form of octaethylporphyrinatonicel.<sup>23</sup> In these two compounds, the greatest angles between pyrrole rings are then 20.2 and 32.8°, respectively. Distortions were ascribed to molecular packing and to steric constraints.

The striking distortion observed in the present structure

most likely results from the C1 carbon insertion in the chain between N(1) and N(4) pyrroles of the original tetraphenylporphine. Indeed, the geometry around the C1 carbon is consistent with a saturated carbon, but the C11–C1–C5 bond angle is reduced to 99.9 (4)°. This contraction is compensated for by a slight increase of the Ni–N4–C44 bond angle to 130.5 (3)° and by an apparent weakening of the Ni–N4 bond length (Table III).

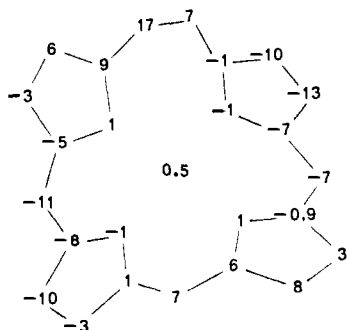


**Figure 3.** Formal diagram to illustrate the distortion of the homoporphyrin skeleton as seen in Figure 1. Each atom symbol has been replaced by its perpendicular displacement, in units of 0.1 Å, from the (4N) plane.

**Table IV.** Least-Square Planes in the Form  $Ax + By + Cz - D = 0$

Planes and Deviations (Å) <sup>a</sup>	
Plane (4N): N1, N2, N3, N4	Plane (Ph5): C51–C56
N1 0.166 (4)	C51 0.006 (5)
N2 -0.160 (4)	C52 -0.005 (5)
N3 0.158 (4)	C53 0.001 (6)
N4 -0.142 (4)	C54 0.002 (6)
Ni 0.054 (1) <sup>b</sup>	C55 0.001 (6)
	C56 -0.006 (6)
Plane (N1): N1, C11–C14	C5 0.064 (4) <sup>b</sup>
N1 -0.010 (4)	Plane (Ph6): C61–C66
C11 0.011 (6)	C61 0.008 (6)
C12 -0.002 (7)	C62 -0.011 (7)
C13 -0.010 (7)	C63 0.007 (8)
C14 0.014 (6)	C64 -0.002 (8)
Plane (N2): N2, C21–C24	C65 0.005 (9)
N2 0.002 (4)	C66 -0.011 (8)
C21 -0.011 (5)	C6 -0.002 (5) <sup>b</sup>
C22 0.020 (6)	Plane (Ph7): C71–C76
C23 -0.017 (7)	C71 0.003 (5)
C24 0.004 (5)	C72 -0.004 (6)
Plane (N3): N3, C31–C34	C73 0.003 (6)
N3 0.018 (4)	C74 -0.001 (6)
C31 -0.031 (6)	C75 0.002 (7)
C32 0.027 (6)	C76 -0.004 (6)
C33 -0.009 (6)	C7 -0.040 (5) <sup>b</sup>
C34 -0.012 (6)	Plane (Ph8): C81–C86
Plane (N4): N4, C41–C44	C81 0.003 (5)
N4 -0.035 (4)	C82 0.004 (6)
C41 0.041 (5)	C83 -0.004 (3)
C42 -0.012 (5)	C84 0.014 (7)
C43 -0.027 (5)	C85 -0.005 (6)
C44 0.046 (5)	C86 -0.003 (6)
	C8 0.041 (4) <sup>b</sup>

	Equations			
	A	B	C	D
(4N)	0.383	-0.842	-0.379	1.183
(N1)	0.315	0.937	0.144	0.794
(N2)	-0.288	0.945	-0.152	-2.404
(N3)	0.723	-0.647	-0.238	2.485
(N4)	0.614	-0.406	-0.676	1.940
(Ph5)	0.288	0.608	-0.739	-0.728
(Ph6)	-0.872	0.145	-0.466	-4.743
(Ph7)	0.611	-0.110	-0.783	0.747
(Ph8)	0.259	0.611	0.747	2.285

Angles (deg) between the Planes			
(4N)–(N1)	43.6	(N1)–(N2)	39.3
(4N)–(N2)	31.9	(N2)–(N3)	38.3
(4N)–(N3)	24.0	(N3)–(N4)	29.6
(4N)–(N4)	33.4	(N4)–(N1)	73.4
		(N1)–(N3)	65.6
		(N2)–(N4)	62.7

<sup>a</sup> All planes are unweighted. <sup>b</sup> Atoms not included in the computation.

**Table V.** Some Selected Intramolecular Contacts (Å)

Ni...C11	2.900 (7)	N1...N2	2.615 (7)
Ni...C14	2.927 (4)	N2...N3	2.640 (4)
Ni...C21	2.906 (4)	N3...N4	2.763 (5)
Ni...C24	2.923 (5)	N4...N1	2.790 (5)
Ni...C31	2.923 (4)		
Ni...C34	2.922 (5)	N1...C1	2.502 (8)
Ni...C41	2.894 (4)	N1...C6	2.443 (7)
Ni...C44	3.070 (4)	N2...C6	2.460 (4)
		N2...C7	2.452 (5)
O1...Ni	2.938 (6)	N3...C7	2.442 (5)
O1...N1	3.129 (5)	N3...C8	2.439 (5)
O1...N4	3.367 (6)	N4...C5	2.471 (8)
		N4...C8	2.461 (8)

Another feature of this structure is the virtual planarity of the nickel and coordinated nitrogen atoms. Thus, the coordination of the nickel atom can be considered as essentially square-planar, involving N1 to N4 atoms of the four pyrrole bases. The Ni–N4 bond length of 1.961 (3) Å is longer than the other three which are equal to  $1.886 \pm 0.010$  Å. As Collins and Hoard point out,<sup>24</sup> the normal Ni–N bond length for diamagnetic square-planar Ni(II) ions varies from 1.84 to 1.92 Å, depending on stereochemical constraints. In an undistorted metalloporphyrin, the normal radius of the “hole” has been estimated to be 2.01 Å.<sup>1,24</sup> Thus, to accommodate an undersized ion like Ni(II), the porphyrinato core must contract. Hoard<sup>25</sup> had postulated that 1.96 Å is the smallest radius in a porphyrin to still retain a planar macrocycle, and then a shortest value must induce distortion from planarity. First the average Ni–N bond length was found to be 1.96 Å in planar nickel porphyrins: 1.957 (13) Å in nickel(II) etioporphyrin I,<sup>17</sup> 1.96 (1) Å in nickel(II) deuteroporphyrin IX,<sup>18</sup> and 1.958 (2) Å in the triclinic form of octaethylporphyrinatonicel.<sup>20</sup> Secondly the shortest Ni–N bond lengths yet observed are 1.929 (3) Å in the tetragonal form of octaethylporphyrinatonicel<sup>23</sup> and 1.908 (5) Å in dihydroporphyrinatonicel.<sup>26</sup> The latter two compounds are both effectively distorted and nonplanar.

While the present compound is actually a nickelhomoporphyrin but not a common nickelporphyrin, this work seems as well to confirm Hoard's theory. The extremely short Ni–N bonds of  $1.886 \pm 0.010$  Å compare closely with those in some nickel(II) corrin complexes (1.83–1.90 Å).<sup>27,28</sup>

Another measure of the distortion is the distance between adjacent pyrrole nitrogen atoms. The N–N distances here vary from 2.615 (7) to 2.790 (5) Å (Table V). For comparison, the average distance is 2.915 Å in the free base tetraphenylporphyrine,<sup>14</sup> 2.768 Å in the planar triclinic form of octaethylporphyrinatonicel,<sup>20</sup> and 2.697 Å in the nonplanar dihydroporphyrinatonicel.<sup>26</sup>

The atoms of the interior ring of the homoporphyrin skeleton form a  $\pi$ -delocalized system: C11, N1, C14, . . . , N4, C44, C5. This electronic system is not cyclic because of the saturated carbon atom C1. Although the atoms of this system do not lie in a plane, the bonding about the carbon atoms is in each case planar (sum of the bond angles equals 360°). Using Ca and Cb to denote the respective  $\alpha$ - and  $\beta$ -carbon atoms of a pyrrole ring, the averaged values for bond lengths in the homoporphyrin skeleton are N–Ca = 1.373 (10), Ca–Cb = 1.433 (10), and Cb–Cb = 1.341 (11) Å, wherein the number in parentheses is the greatest value of the estimated standard deviation for an individually determined length. It appears that the Cb–Cb bonds correspond closely in length to double bonds and that the eight Cb carbon atoms are isolated from the inner system. However, this is perhaps a result of the C–H bond densities which induce an apparent shortening of the C–C bond

Table VI. Interatomic Distances less than 3.70 Å<sup>a</sup>

N2...C62	2/001	3.567 (9)	C65...C32	1/011	3.642 (12)
C12...C85	1/001	3.559 (11)	C65...C4	1/011	3.692 (9)
C21...C62	2/001	3.610 (9)	C72...N3	2/000	3.578 (10)
C24...C62	2/001	3.689 (11)	C72...C31	2/000	3.612 (9)
N3...C72	2/000	3.578 (10)	C73...N3	2/000	3.498 (9)
N3...C73	2/000	3.498 (9)	C73...C34	2/000	3.620 (9)
C31...C72	2/000	3.612 (9)	C74...C54	1/111	3.698 (9)
C32...C65	1/011	3.642 (12)	C74...C83	1/110	3.659 (6)
C34...C73	2/000	3.620 (9)	C74...C86	2/000	3.687 (8)
C42...C85	2/110	3.607 (10)	C82...C56	2/100	3.648 (10)
C43...C52	2/111	3.650 (7)	C83...C74	1/110	3.659 (6)
C43...C4	2/100	3.652 (12)	C85...C12	1/001	3.559 (11)
C52...C43	2/111	3.650 (7)	C85...C42	2/110	3.607 (10)
C54...C74	1/111	3.698 (9)	C86...C74	2/000	3.687 (8)
C56...C82	2/100	3.648 (10)	O1...C63	2/001	3.280 (6)
C62...N2	2/001	3.567 (9)	C4...C43	2/100	3.652 (12)
C62...C21	2/001	3.610 (9)	C4...C65	1/011	3.692 (9)
C62...C24	2/001	3.689 (11)	C9...C64	2/001	3.646 (31)
C63...O1	2/001	3.280 (6)			

<sup>a</sup> Second atoms not in the crystal chemical unit (*i.e.*, not listed in Table I) are specified by the code *I/uvw* which denotes the manner in which the atomic parameters can be derived from the corresponding atom in the crystal unit. *I* refers to one of the following symmetry operations: (1) *xyz*; (2)  $\bar{x}\bar{y}\bar{z}$ . The *u,v,w* digits code a lattice translation as  $ua + vb + wc$ .

lengths as observed and described by Collins, *et al.*<sup>29</sup> Further support of this argument is also provided by the relatively short lengths of the Ca–Cb bonds. Examination of the N–Ca bonds shows two individual bond lengths, N1–C11 = 1.336 (10) and N4–C14 = 1.409 (10) Å, which markedly differ from the others. It is interesting to note that these bonds affect the (N1) and (N4) pyrroles. These differences can be attributed to a weakening of  $\pi$ -delocalization at the extremities of the  $\pi$ -delocalized system. Nevertheless the N1–C11 bond is quite short and its length probably underestimated.

The phenyl groups are independently planar and tilted with respect to the plane of the three neighboring carbons of the bridge positions between pyrroles. The tilted angles of the four phenyls Ph(5) to Ph(8) are 46.4, 79.3, 63.9, and 60.6°, respectively (Table IV). Finally, the phenyl groups are bound to the bridge positions through apparently shortened single bonds and appear to be electronically isolated from the inner system.

The plane defined by C5, C1, and C11 carbon atoms makes a dihedral angle of 80.6° with the (4N) plane. The ester group is bound to C1 so that it lies above the (4N) plane toward the nickel atom. That well agrees with the expected endo structure. The O1 ester oxygen approaches the nickel at a distance of 2.938 (6) Å and some little interaction can occur with the metal.

Many contacts exist between successive overlying mole-

cules (Table VI). The closest of these involving atoms of the homoporphyrin skeleton range upwards from 3.280 (6) Å for C...O, 3.559 (11) Å for C...C, and 3.498 (9) Å for C...N distances. The shortest packing separation, 3.28 Å, is between the C63 phenyl carbon and the O1 oxygen of the ester function. Methylene chloride is present in the crystal as the uncomplexed solvent of crystallization and provides only weak contacts with neighboring molecules.

**Acknowledgment.** We would like to thank Dr. H. J. Callot for the gift of the products and for helpful discussions.

**Supplementary Material Available.** A listing of structure factor amplitudes will appear following these pages in the microfilm edition of this volume of the journal. Photocopies of the supplementary material from this paper only or microfiche (105 × 148 mm, 24× reduction, negatives) containing all of the supplementary material for the papers in this issue may be obtained from the Journals Department, American Chemical Society, 1155 16th St., N.W., Washington, D.C. 20036. Remit check or money order for \$4.00 for photocopy or \$2.00 for microfiche, referring to code number JACS-75-1416<sup>7</sup>

## References and Notes

- (1) J. L. Hoard, *Science*, **174**, 1295 (1971).
- (2) J.-H. Fuhrhop, *Angew. Chem.*, **86**, 363 (1974).
- (3) D. Ostfeld and M. Tsutsui, *Accounts Chem. Res.*, **7**, 52 (1974).
- (4) H. J. Callot and Th. Tschamber, *Tetrahedron Lett.*, 3155, 3159 (1974).
- (5) R. Grigg, *J. Chem. Soc. C*, 3664 (1971).
- (6) Preliminary communication, *J. Chem. Soc., Chem. Commun.* 884 (1974).
- (7) W. R. Busing, "Crystallographic Computing," F. R. Ahmed, Ed., Munksgaard, Copenhagen, 1970, p 319.
- (8) W. R. Corfield, R. J. Doedens, and J. A. Ibers, *Inorg. Chem.*, **6**, 197 (1967).
- (9) "International Tables for X-Ray Crystallography," Vol. III, Kynoch Press, Birmingham, 1962, p 215.
- (10) D. T. Cromer and J. T. Waber, *Acta Crystallogr.*, **18**, 104 (1965).
- (11) C. T. Prewitt, "A Fortran IV Full-Matrix Crystallographic Least-Squares Program," SFLS 5, 1966.
- (12) See paragraph at end of paper regarding supplementary material.
- (13) V. Schomaker, J. Waser, R. E. Marsh, and G. Bergman, *Acta Crystallogr.*, **12**, 600 (1959).
- (14) S. J. Silvers and A. Tulinsky, *J. Amer. Chem. Soc.*, **89**, 3331 (1967).
- (15) B. M. L. Chen and A. Tulinsky, *J. Amer. Chem. Soc.*, **94**, 4144 (1972).
- (16) J. W. Lauher and J. A. Ibers, *J. Amer. Chem. Soc.*, **95**, 5148 (1973).
- (17) E. B. Fleischer, *J. Amer. Chem. Soc.*, **85**, 146 (1963).
- (18) T. A. Hamor, W. S. Caughey, and J. L. Hoard, *J. Amer. Chem. Soc.*, **87**, 2305 (1965).
- (19) E. B. Fleischer, C. K. Miller, and L. E. Webb, *J. Amer. Chem. Soc.*, **86**, 2342 (1964).
- (20) D. L. Cullen and E. F. Meyer, Jr., *J. Amer. Chem. Soc.*, **96**, 2095 (1974).
- (21) M. B. Hursthouse and S. Neidle, *J. Chem. Soc., Chem. Commun.*, 449 (1972).
- (22) G. M. McLaughlin, *J. Chem. Soc. Perkin Trans. 2*, 136 (1974).
- (23) E. F. Meyer, Jr., *Acta Crystallogr., Sect. B*, **28**, 2162 (1972).
- (24) D. M. Collins and J. L. Hoard, *J. Amer. Chem. Soc.*, **92**, 3761 (1970).
- (25) J. L. Hoard, *Ann. N. Y. Acad. Sci.*, **206**, 18 (1973).
- (26) P. N. Dwyer, J. W. Buchler, and W. R. Scheidt, *J. Amer. Chem. Soc.*, **96**, 2789 (1974).
- (27) M. Dobler and J. D. Dunitz, *Helv. Chim. Acta*, **54**, 90 (1971).
- (28) M. Currie and J. D. Dunitz, *Helv. Chim. Acta*, **54**, 98 (1971).
- (29) D. M. Collins, W. R. Scheidt, and J. L. Hoard, *J. Amer. Chem. Soc.*, **94**, 6689 (1972).